1

High-Order Harmonic Studies of the Role of Resonances on the Temporal and Efficiency Characteristics of Converted Coherent Pulses: Different Approaches

1.1 Resonance Harmonic Generation in Gases: Theory and Experiment

Excitation of atomic resonances exhibits a simple way to enhance high-order harmonic conversion efficiencies. The basic idea is straightforward: the driving laser is tuned to an atomic resonance (usually a multiphoton resonance, e.g. with n photons from the driving laser involved). The resonance enhances the nonlinear susceptibility $\chi^{(n)}$ of order n. If permitted by selection rules, this supports generation of the nth harmonics of the driving laser or frequency mixing processes with m additional photons from the same laser field, e.g. generating harmonics of order $(n + m)$. Such resonantly enhanced frequency conversion is well known from low-order frequency conversion processes, driven by lasers of moderate intensities. As a simple example, one can note resonantly enhanced four-wave mixing in atomic gases. Here, a first laser pulse drives a two-photon transition, which serves to resonantly enhance a sum or difference frequency mixing process with a second laser pulse. However, during initial studies of this process it was not obvious, that resonance enhancement occurs for generation of high-order harmonics driven by high-intensity ultrashort laser pulses.

The strong electric field of the laser significantly perturbs the level structure of the medium and may destroy any resonance effect in conversion processes. From this simple consideration it becomes clear, that resonantly enhanced harmonic generation with ultra short pulses may be efficient, if the driving radiation field is, on one hand, sufficiently strong to drive high-order harmonic generation (HHG), and on the other hand the field is still not too strong to destroy the resonance structure of the medium. In the terminology of high intensity laser–matter interactions and photoionization, one can consider operation in the regime of "multi-photon ionization" rather than "tunneling ionization" (see Ref. [1] and references therein). This choice provides appropriate conditions to observe pronounced resonance effect. The restriction toward not-too-strong laser intensities still enables a large range of applications and the possibility to exploit resonances for efficient harmonic generation. One can

Resonance Enhancement in Laser-Produced Plasmas: Concepts and Applications,
First Edition. Rashid A. Ganeev.

also note that proper investigation and application of resonance effects also requires tunable lasers and moderate frequency bandwidth (i.e. not-too-short pulse durations) to properly address isolated atomic and ionic resonances.

There are only few studies of resonance enhancement in harmonic generation in gases via bound atomic states (for example, [2, 3]). The enhancement of particular harmonics in those studies was observed at specific laser intensities, which allowed an increase in the yield of the *n*th harmonic by exciting a dynamically shifted *n*-photon resonance. Another consideration of this enhancement was suggested in Ref. [4], where the phase-matching effects or multiphoton resonances were attributed for the harmonic enhancement. Contrary to gases, a sequence of experiments on pronounced enhancement of single harmonics in laser-driven plasmas [5] has shown that this effect is attributed to dynamically shifted ionic resonances close to specific harmonics. The details of latter studies will be discussed in the following chapters. Notice that in most cases only single harmonics were enhanced, while the theoretical predictions show that excitation of *n*-photon resonances should also affect harmonics with order larger than *n* [6–8]. The resonance HHG can also be realized through atomic Fano resonances [9].

In Ref. [1], the coupling scheme and relevant energy levels in a jet of argon atoms were considered (see Figure 1.1). The intense picosecond laser pulses were in the vicinity of the five-photon resonance $3p^6\,{}^1S_0 \rightarrow 4s,\ [1/2]_1$ at 95 400 cm^{-1}, corresponding to a fundamental laser wavelength of 524 nm. In the experiment, the resonantly enhanced 5th harmonic generation of the driving laser radiation as well as harmonics of higher order (indicated by dashed arrows in the figure) were observed. The authors investigated harmonic generation in a dense Ar gas jet driven in the vicinity of above resonance by intense tunable picosecond radiation pulses from dye amplifier system. The laser system combined sufficient intensity (i.e. up to 100 TW cm^{-2}) to approach the regime of HHG with still fine spectral resolution to address and exploit single atomic resonances. In a first experiment on resonantly enhanced 5th harmonic generation, they determined pronounced AC-Stark shifts and line broadenings of the five-photon resonance. Moreover, they found evidence for an additional difference frequency mixing process "six minus one photon" via a set of highly excited states in Ar, which also generates radiation at the 5th harmonic of the driving laser. In a second experiment, they investigated the effect of resonant multiphoton excitation on the generation of harmonics (i.e. with higher order than the involved multiphoton transition). When the laser frequency was tuned to the Stark-shifted five-photon resonance, a pronounced resonance enhancement was found not only of the 5th, but also of the 7th and 9th harmonic. They pointed out that, as an important feature of resonance enhancement, the laser wavelength must be matched to the position of the Stark-shifted atomic resonance, which depends upon the applied laser

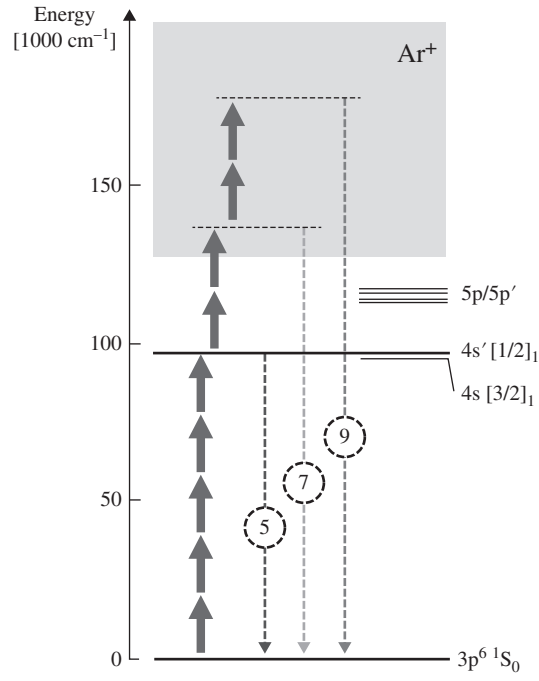

Figure 1.1 Coupling scheme in argon atoms with relevant energy levels. The short designation (5p/5p′) indicates the manifold of closely spaced states 5p′ $[3/2]_2$, 5p $[1/2]_0$, 5p $[3/2]_2$, and 5p $[5/2]_2$. Full arrows depict the driving laser at 524 nm, dashed arrows indicate the 5th, 7th, and 9th harmonics, as investigated in the experiment. *Source:* Ackermann et al. 2012 [1]. Reproduced with permission from Optical Society of America.

intensity. The experimental data clearly demonstrate the effect of resonant multiphoton excitation to enhance harmonic generation.

Resonantly enhanced harmonic generation is a particular example of the more general HHG technique. Although resonantly enhanced HHG has been shown to increase the harmonic yield in a limited range of settings, it has more recently been explored for its potential to reveal the dynamics of bound and quasi-bound states in the presence of a strong driving field [10–16]. Several mechanisms for resonant enhancement have been discussed in the literature, generally all involving an intermediate, resonant step in the semiclassical model. The resonant step may occur either in the ionization process, via a multiphoton resonance between the ground state and the Stark-shifted excited state, or in the rescattering process via enhanced recombination, or by capture into an excited bound state that subsequently decays via spontaneous emission of light. The capture and spontaneous emission process has been explored in detail for short-lived quasi-bound states embedded in a continuum, for which it can give rise to very large enhancements [10, 13]. For bound-state resonances with long lifetimes, the capture and spontaneous emission process can generally be distinguished from the coherently driven resonant enhancement (via multiphoton ionization or enhanced recombination), since it will give rise to narrow-band radiation at the field-free resonance frequency, given that it

largely takes place after the driving laser pulse is over [13]. More details on the theoretical models of the resonant enhancement of HHG will be discussed in the following chapter.

In contrast to this, the coherently driven resonantly enhanced response will give rise to emission at the difference frequency between the ground state and the Stark-shifted excited state since this process only takes place while the laser field is on. The coherently driven resonance-enhanced harmonic generation and investigation of the interplay between the resonant enhancement and the quantum path dynamics of the harmonic generation process is of utmost interest to understand the peculiarities of this process. In particular, authors of Ref. [17] have studied how the amplitude and phase of the different quantum path contributions to the harmonic yield in helium are changed in the vicinity of a bound-state resonance. They presented a study of the interplay between resonant enhancement and quantum path dynamics in near-threshold harmonic generation in helium and analyzed the driven harmonic generation response by time-filtering the harmonic signal so as to suppress the long-lasting radiation that would result from population left in excited states at the end of the pulse. By varying the wavelength and intensity of the near-visible driving laser field, they identified a number of direct and indirect enhancements of H7, H9, and H11 via the Stark-shifted 2p–5p states. For H9, the Autler–Townes-like splitting of the enhancement was observed due to the 3p state, when the wavelength and intensity are such that the driving field strongly couples the 3p state to the nearby dark 2s state.

In was found, in terms of the quantum path dynamics, that both the short- and the long-trajectory contributions to the harmonic emission can be easily identified for harmonics that are resonantly enhanced via the Stark-shifted *n*p states. The authors of Ref. [17] found that both contributions are enhanced on resonance and that the maximum of the envelope of the resonant harmonic is delayed by approximately 0.5 optical cycles. It was interpreted to mean that the enhancement happens via a multiphoton resonance between the ground state and the Stark-shifted excited state and that the electron is then trapped for a while in the excited state before entering the continuum. Furthermore, they found that only the long-trajectory contribution acquires a phase shift, which leads to a delay in emission time of approximately 0.125 optical cycles, suggesting that the phase shift is acquired in the interaction between the returning electron wave packet and the ion core, for which there is a large difference in the short- and long-trajectory dynamics. Finally, they have shown that both the enhancement and the phase shift are still visible in the macroscopic response. This means that these effects could potentially be explored experimentally, especially considering that the calculations predict that the macroscopic response is dominated by the long-trajectory contribution, which exhibits the on-resonance phase shift.

Some experiments have considered an interesting alternative for lower intensities below 10^{14} W cm^{-2}. Authors of Ref. [3] note atomic resonance effects on the 13th harmonic for argon in a Ti:sapphire field. Theoretically, there have been investigations of model systems in which resonant enhancement of harmonic generation has been noted. Plaja and Roso [18] have demonstrated that HHG resonant structures occur in a two-level atom when AC-Stark-shifted level energies (the real parts of the complex Floquet quasi-energies discussed in Refs. [19, 20]) undergo avoided crossings. Gaarde and Schafer [7] have performed one-electron pseudo-potential calculations modeling potassium in a Gaussian laser pulse, which shows resonant enhancement of harmonics. In Ref. [20], theoretical predictions of resonance enhanced harmonic generation for argon in a KrF laser field, which take full account of atomic structure effects, are presented. These are ab initio calculations with no empirical adjustable parameters. They have described how the resonant behavior of the harmonics arises from the interaction between quasi-energies. The mechanisms and general features of their results could be applied to general atomic resonances in laser fields.

Another approach is related with the influence of plasmonic resonances on the harmonic efficiency. Particularly, the study [21] was devoted to numerical simulations of the laser–cluster interaction with emphasis on the nonlinear collective electron dynamics and the generation of low-order harmonics in a comparatively small cluster consisting of $\sim 10^3$ atoms. The classical molecular-dynamics simulation model taken into account almost all of the ingredients of the laser–cluster interaction. In full qualitative agreement with the phenomenological picture of nonlinear oscillations of a cloud of electrons trapped inside a charged cluster in a strong laser field [22–24], they have observed a strong 3rd harmonic excitation when the tripled laser frequency became close to the Mie frequency that is, near the third-order resonance with the Mie frequency. This corresponds to nonlinear excitation of the dipole surface plasmon. The resonant behavior can be seen both in the total electron acceleration (which is responsible for 3rd harmonic generation by the cluster) and in the internal electric field of the cluster (which is responsible for ionization of the cluster constituents). Varying the laser wavelength produces a pronounced resonance curve whose width affords an estimate of the width of the Mie resonance in a cluster irradiated by a strong laser field. The time-dependent envelopes of the total electron acceleration and of the inner electric field at the position of the central cluster ion have been calculated at the fundamental frequency and at the 3rd harmonic. They have confirmed the presence of the 3rd harmonic (and of higher harmonics, especially the 5th) in the total electron acceleration as well as in the inner electric field at the position of the central ion and its resonant behavior when the frequency of the incident laser sweeps through the corresponding nonlinear resonance with the time-dependent Mie frequency. The dependence of the

time-dependent yield of the 3rd and 5th harmonics on the various parameters of the laser–cluster interaction was analyzed.

Basically, the described approaches require one-photon resonance for fundamental and generated radiations. The claimed primary implementation of such studies is to extend the generated radiation to the extreme ultraviolet (XUV) range where the efficiency to be achieved exceeds that in crystals. Therefore, the coupling of the generated XUV radiation and fundamental radiation becomes almost inevitable for achieving large enhancement of harmonic yield.

Although HHG via interaction of intense laser pulses with matter provides a unique source of coherent femtosecond and attosecond pulses in the XUV, the low efficiency of the process is a serious limit to its wide application. Using the resonances of the generating medium is a natural way to boost the efficiency, as was already suggested in early HHG experimental [3] and theoretical [18, 25] studies. Generation of high harmonics with frequencies close to that of the transition from the ground state to an autoionizing state (AIS) of the generating particle was experimentally investigated in plasma media [26] and in noble gases [27]. A number of theories describing HHG enhancement based on the specific properties of AIS were developed [10, 28–30]. These theories involve the rescattering model in which the HHG is described as a result of tunneling ionization, classical free electronic motion in the laser field, and recombination accompanied by the XUV emission upon the electron's return to the parent ion. In particular, in Ref. [10] a four-step resonant HHG model was suggested. The first two steps are the same as in the three-step model, but instead of the last step (radiative recombination from the continuum to the ground state) the free electron is trapped by the parent ion, so that the system (parent ion + electron) lands in the AIS, and then it relaxes to the ground state emitting XUV. In addition, there are several theoretical studies in which the HHG efficiency was calculated using the recombination cross-section. It was done heuristically [31] and analytically [32] for the Coulomb interaction and by generalizing the numerical results for the molecules [33].

In Ref. [34], the HHG theory considering an AIS in addition to the ground state and the free continuum treated in the theory for the nonresonant case was suggested. They have shown that such accurate consideration verifies the model [10]. Moreover, they have shown that the intensity of the resonant HHG is described with a Fano-like factor that includes the scattering cross-section. However, in contrast to previously suggested theories, this approach also allows calculating the resonant harmonic's phase. Their theory generalizes the strong-field approximation approach for HHG to the resonant case, considering an AIS in addition to the ground state and the free continuum state; the latter two states are treated in the same way as in the theories developed for the nonresonant case. This theory allows calculating not only the resonant harmonic intensity but also its phase. It was shown that there is a rapid variation of the phase in the vicinity of the resonance. These calculations

reasonably agree with the RABBIT harmonic phase measurements. The theory predicts that in the case of a resonance covering a group of harmonics the resonance-induced phase variation can compensate for the attochirp in a certain spectral region. In the following we discuss one of their results.

The calculated spectrum of the resonant 17th harmonic from Sn plasma calculated using the numerical time-dependent Schrödinger equation (TDSE) solution as described in Ref. [35] averaged for laser intensities up to 0.8×10^{14} W cm^{-2} is shown in Figure 2.1. The laser pulse duration is 50 fs. One can see that different detuning from the resonance led to different peak harmonic intensities and, even more interesting, to different harmonic line shapes: for the 793, 796, and 808 nm fundamentals the harmonic line consists of two peaks. It is known for the nonresonant HHG that these peaks can be attributed to the contributions of the short and the long electronic trajectories. In Figure 1.2 one can see that the long trajectory's contribution is, in general, weak, but it becomes more pronounced when its frequency is closer to the exact resonance, as is the case for the 793 nm fundamental. These results illustrate the fact that the harmonic line shape can be well understood via the factorization of the harmonic signal. This straightforward factorization is a remarkable fact, considering the complexity of the dynamics of both the free electronic wave packet and the AIS, which determine the harmonic line shape.

Attosecond pulse production using high-order harmonics generated by an intense laser field [36, 37] is essentially based on the phase locking of the

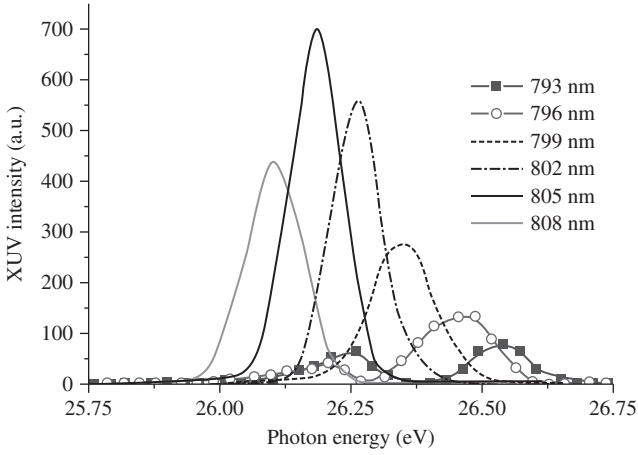

Figure 1.2 The calculated harmonic spectrum in the vicinity of the resonance for different fundamental wavelengths, leading to different detunings from the resonance. The resonant transition is the $4d^{10}5s^25p\ ^2P_{3/2} \leftrightarrow 4d^95s^25p^2\ (^1D)_2\ D_{5/2}$ transition in Sn^+; the transition frequency is 26.27 eV, which is close to the 17th harmonic of a Ti:sapphire laser. *Source:* Strelkov et al. 2014 [34]. Reproduced with permission from American Physical Society.

harmonics. This phase locking is well understood [38] for the case when there are no resonances affecting the process. However, recently much attention has been paid to the role of resonances in HHG in gases and plasma plumes. It was shown that when the high-harmonic frequency is close to the transition to an excited quasi-stable state of the generating particle, the harmonic can be much more intense than the off-resonant ones. For the HHG in plasma plumes such an enhancement can be as high as an order of magnitude greater.

An enhancement of the efficiency of XUV generation due to giant resonance in Xe was predicted in Ref. [29] and observed in Refs. [12, 39]. Namely, the XUV in the spectral region of about 20 eV is more intense than the lower frequency XUV, and the enhancement near the center of the resonance is approximately an order of magnitude.

Broadband resonant enhancement potentially allows generating attosecond pulses using resonant harmonics. This approach is interesting not only because of the higher generation efficiency of the resonant HHG, but also because it essentially reduces the requirements for harmonic filtering (the resonant region naturally stands out). However, phase locking of resonant HHG differs from the one of nonresonant HHG, so attosecond pulse production in the former case is not straightforward. In Ref. [40], this aspect of resonant HHG was investigated both numerically and analytically. The effect of resonance on the phase difference between the neighboring harmonics was studied, which allowed calculating the duration of the attosecond pulses produced by resonant harmonics. The conditions were found for which the free-motion-induced attochirp can be compensated by the resonantly induced attochirp, leading to phase synchronization of a group of resonant harmonics. It was shown that attopulses with a duration of 165 as can be obtained using resonantly enhanced harmonics generated in Xe. This duration is smaller than the minimal duration of the attosecond pulse formed by the off-resonant harmonics; it can be further reduced down to almost a hundred attoseconds using the two-color driver. Resonant HHG enhancement leads to an increase of the attopulse intensity by more than an order of magnitude and relaxes the requirements for XUV filtering: only harmonics much lower than the resonance should be suppressed by the filter.

Conversion efficiency is the most important parameter in HHG, and many other schemes have been proposed to improve the conversion efficiency. In theory, using excited atoms with Rydberg states was proved to be an effective way to generate harmonics with both large cutoff energy and high conversion efficiency [41–44]. In experiment, Paul et al. [45] reported on the observation of enhanced HHG from the excited Rb vapor with resonance excitation by using a weak diode laser. However, there were almost no experimental reports on the enhanced HHG from the excited atoms of rare gas with Rydberg states. The experimental demonstration of the enhanced HHG from optically prepared excited atoms with Rydberg states, which is different from resonance excitation and can be created by tunneling ionization [46–48], was recently

demonstrated in Ref. [49]. They used an effective pump-probe scheme to experimentally demonstrate the enhanced HHG from a superposition state of ground state and excited states in argon. In their experiment, an obvious enhancement plateau of HHG with a half lifetime of dozens of picoseconds is observed when controlling the time delay between the pump and probe laser pulse, and the harmonic intensity is enhanced by nearly 1 order of magnitude compared to the case without pre-excitation. Then, the gradual enhancement process is demonstrated with the increasing intensity of pump pulse for improving the population of excited states. A theoretical simulation with excited populations by solving TDSE well explained those experimental results.

1.2 Role of Resonances in Plasma Harmonic Experiments: Intensity and Temporal Characterization of Harmonics

A breakthrough in this area of studies was reported in Ref. [50] where strong resonant enhancement in HHG from low-ionized indium plasma was experimentally demonstrated, which was attributed to the superposition of ground state and excited states [28, 51, 52]. The results, which constitute the first temporal characterization of the femtosecond envelope of the resonant high-order-harmonic emission from ablation plasma plumes, were discussed in Ref. [53]. The complex nature of this medium containing different kinds of ions and a rather high free electron density does not allow relying on straightforward analogies with the well-known HHG in neutral gases. The confirmation, found in their results, that the XUV emission from indium plasmas, both resonant and nonresonant, has a femtosecond envelope thus constituting an important advance. While the determined harmonic pulse durations bear significant relative uncertainties, they consistently found XUV pulse durations that are shorter than the driving laser pulse for all plasma targets.

While those results for the resonance-enhanced harmonics are not yet conclusive with regard to Strelkov's four-step model, they give new experimental input to the theoretical effort of modeling. The surprising similarity of the pulse envelope for resonant and nonresonant harmonics is very good news which, in view of the very high conversion efficiencies of 10^{-4} observed in other experiments with indium plasma, opens the perspective of a very high peak flux tabletop XUV source. The central wavelength of these pulses could be selected by choosing a target material with a strong transition at the desired energy. These measurements could be complemented by more advanced temporal characterization. For instance, in so-called XFROG measurements, using

a shorter infrared (IR) probe pulse, such that $\tau_{XUV} > \tau_{IRprobe}$, would allow a more precise determination of the XUV pulse duration as well as a measurement of the harmonic chirp rate, as demonstrated in Ref. [54]. Alternatively, a high-order harmonic SPIDER measurement would give direct access to both temporal envelope and phase. Finally, a complete characterization of the harmonic emission including its attosecond (sub)structure with the FROG–CRAB method [55] would of course be the most desirable progress, albeit certainly also the most challenging one. All of these would give information on the intensity dependence of the harmonic phase, which may be different for resonant and nonresonant harmonics, thus shedding more light on the mechanism behind resonant enhancement.

Major efforts up to now have been devoted to increasing the photon flux of resonant harmonics. However, there have only been a few experiments that were aimed for better understanding of the physics involved behind this resonant harmonics generation. These experiments have only shown that the resonant harmonics intensity depends strongly on the ellipticity of the driving laser [56], and follows phase-matching conditions similar to other conventional gas harmonics [57].

Experimentally observed intensity enhancements of resonance harmonics have been compared with theory for several materials [10], and the relative phase between resonant harmonics and nonresonant harmonics have been experimentally measured and compared with theory [51]. However, intensity and phase measurements of the harmonics are still indirect evidence of the four-step model, and thus there currently lacks direct and concrete evidence that the AIS is involved in resonant harmonics generation. In Ref. [58], the electron quantum paths in the vicinity of AIS with mid-IR tunable driving fields were studied. Those results allow to unambiguously clarify the mechanism involved in resonance harmonics generation. The study has shown that resonant harmonics generation process involves the AIS for coherent harmonic emission at resonant energy via the microscopic response. Further, it has been revealed that the resonant harmonics generation process involves the dressed AIS for coherent harmonic emission at frequencies $\pm 2\Omega$ from the resonant harmonic frequency (Ω represents laser frequency). As resonant harmonic is an excellent candidate as a source for intense harmonics, the involvement of dressed states in HHG opens the perspective to expand the bandwidth of those harmonics (for example, one can generate harmonics at $\pm 2\Omega$, $\pm 4\Omega$, and above frequencies), thus opening the possibility to generate intense and ultrashort attosecond pulses, useful for the applications of attosecond science [59, 60]. The direct involvement of AIS in resonant harmonics generation via microscopic response will also provide opportunities to study emission dynamics of AIS with ultrafast lasers. For example, one can extract information about the absolute time that the electron stays in the AIS before emission, study electron–electron interaction, and interference of resonant

harmonics and direct harmonic at attosecond timescale by driving harmonics using pulses with certain duration, as the electron stays for a short time in the AIS. Further, harmonic emission from virtual quantum states will provide opportunities to understand the nature of virtual states and their influence on the physical systems both in physics and chemistry, hence providing better control on the systems and roots to find new applications.

Previous studies of resonant harmonics generation were focused at a single state (particularly, the AIS for the case of Sn II), which is in the multiphoton resonance with the driving laser [51, 61]. However, experimental observations show that resonant harmonics generation can involve three different states: the actual AIS and the two dressed states located at $\pm 2\Omega$ around the resonant AIS. At the third step of the four-step model the system finds itself in one of these states and then, at the fourth step, it recombines to the ground state and emits one of the three resonant harmonics. It is obvious that when the driving wavelength corresponds to the exact multiphoton resonance, the harmonics from these dressed states overlap with the neighboring nonresonant harmonics, and thus the two are difficult to differentiate. However, these satellite harmonics can be distinguished from each other when the driving wavelength is detuned. Thus, this observation shows that the driving wavelength detuning from the resonance allows to observe the very pronounced separation of resonance harmonic and driving harmonic, as well as the spectral peaks generated due to the dressed AIS.

Note that very pronounced enhancement of the harmonics neighbor to the resonant one was found theoretically in Ref. [28]. This theory considers a coherent superposition of ground and excited states formed by pumping by the resonance harmonic, and thus assumes quite high intensity of this harmonic. The moderate intensity of resonant harmonic in the discussed experiments [58] (in general, comparable to the one of the dressed harmonics) prevents the direct application of this theory for their interpretation. Those observations provide the accurate information of the quantum path that the electron follows in the vicinity of the AIS for resonant harmonics generation. It was shown that for resonance harmonic generation the electron quantum path is perturbed not only from the AIS but also from the dressed states, resulting in three coherent harmonic generations. In high-order harmonic attosecond science, pump-probe absorption spectroscopy has been recently started to study the light–matter interaction with dressed AIS [62]. However, the propagation and emission dynamics of the electron from dressed AIS have been highly ignored. The observation of satellite harmonics from dressed AIS shows that the AIS dressing by the laser field should be taken into account to describe also the emission processes during the light–matter interaction for elements containing AIS. As AIS exist in different materials, the discussed work will be applicable in general to study the influence of dressed states on electron quantum path in all these materials. As dressed states respond within the

driving laser pulse, the nonlinear properties of the dressed AIS will provide the opportunity to study and control electronic motion at fast timescales, which will be an advantage as electrons remain in the AIS for only a few hundred attoseconds to a few femtoseconds.

The study [61] gave an affirmative answer to the practical question of whether resonance-enhanced HHG is indeed a source of intense ultrashort XUV pulses. They reported that enhanced harmonic order has the same femtosecond duration as the nonresonant ones. On the attosecond timescale however, they found significant distortions of the phase of the near-resonant harmonic. Those results suggest the detuning from the resonance as an effective handle controlling the resonant harmonic phase. From a more fundamental viewpoint, previous studies of the HHG phase properties focused mainly on the phase accumulated by the quasi-free electron in the continuum, or on the recombination step as a probe of molecular structure and dynamics [63, 64]. The discussed results present experimental evidence of the dramatic influence of the recombination step on the phase of resonant harmonics from the plasma. It was shown that the recombination dipole matrix element alone can describe the origin of the phase distortions observed in the experiments. This is the basis for the so-called "self-probing" schemes to extract structural and dynamic information about the generating system from intensity, phase, and polarization measurements of high-order harmonics. Those results thus suggest the possibility of devising "self-probing" schemes for atomic resonances based on the advanced characterization of resonance-enhanced high harmonics. In particular, the rapid phase variation responsible for the intriguing suppression of the RABBIT oscillations may encode characteristic features of the involved AIS.

Recently, alongside the plasma medium, resonance HHG has been discovered in other systems, for example, in atomic Fano resonances [9] and in SF_6 molecule [65]. Resonance-enhanced HHG introduces the possibility of increasing the conversion efficiency of a specific harmonic by more than an order of magnitude compared to nonresonant HHG in noble gases. If this effect could be combined with phase-matching effects and/or coherent control of HHG, then an intense XUV source could be generated with only a single harmonic in the spectrum. Such a unique radiation source will truly be ideal for accelerating its various applications in physics, chemistry, biology, and for exploring new fields such as nonlinear X-ray optics and in attosecond physics. It would have excellent spatial coherence [66], the possibility of high repetition rate (of the order of kilohertz to hundreds of kilohertz), and improved conversion efficiency.

There are two possible explanations for the mechanism of this resonant harmonic. The most common is based on modified three-step model. However, a second explanation relies on the collective response of the medium instead of the single-atom response, i.e. on the phase-matching conditions [67]. The results reported in Ref. [57] clearly indicate the existence of a

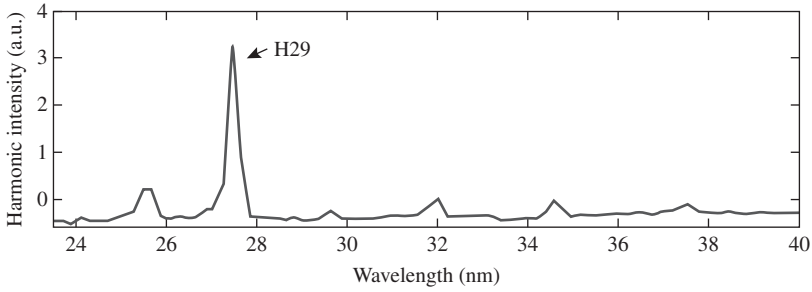

Figure 1.3 Harmonic spectra from chromium plasma including the resonance harmonic (H29). *Source:* Rosenthal and Marcus [57]. Reproduced with permission from American Physical Society.

resonance enhanced harmonic in harmonic spectrum of chromium plasma (Figure 1.3). Nevertheless, analysis of coherence length does not show any dramatic change in the coherence length of that harmonic with respect to the neighboring harmonics. Those results do not support the phase-matching enhancement hypothesis. Rather, they favor the viewpoint that the single atom is responsible. However, the single-atom response is not fully understood, and further investigation must be carried on.

References

1 Ackermann, P., Münch, H., and Halfmann, T. (2012). *Opt. Express* 20: 13824.
2 L'Huillier, A., Balcou, P., and Lompré, L.A. (1992). *Phys. Rev. Lett.* 68: 166.
3 Toma, E.S., Antoine, P., Bohan, A., and Muller, H.G. (1999). *J. Phys. B* 32: 5843.
4 Barkauskas, M., Brandi, F., Giammanco, F. et al. (2005). *J. Electron. Spectrosc. Relat. Phenom.* 144–147: 1151.
5 Ganeev, R.A. (2009). *Phys. Usp.* 52: 55.
6 Taïeb, R., Véniard, V., Wassaf, J., and Maquet, A. (2003). *Phys. Rev. A* 68: 033403.
7 Gaarde, M. and Schafer, K. (2001). *Phys. Rev. A* 64: 013820.
8 de Morisson Faria, C., Kopold, R., Becker, W., and Rost, J. (2002). *Phys. Rev. A* 65: 023404.
9 Rothhardt, J., Hädrich, S., Demmler, S. et al. (2014). *Phys. Rev. Lett.* 112: 233002.
10 Strelkov, V. (2010). *Phys. Rev. Lett.* 104: 123901.
11 Redkin, P.V. and Ganeev, R.A. (2017). *J. Phys. B* 50: 185602.
12 Shiner, A., Schmidt, B., Trallero-Herrero, C. et al. (2011). *Nat. Phys.* 7: 464.

13 Tudorovskaya, M. and Lein, M. (2011). *Phys. Rev. A* 84: 013430.
14 Jin, C., Bertrand, J.B., Lucchese, R.R. et al. (2012). *Phys. Rev. A* 85: 013405.
15 Chu, X. and Groenenboom, G.C. (2013). *Phys. Rev. A* 87: 013434.
16 Xiong, W.-H., Geng, J.-W., Tang, J.-Y. et al. (2014). *Phys. Rev. Lett.* 112: 233001.
17 Camp, S., Schafer, K.J., and Gaarde, M.B. (2015). *Phys. Rev. A* 92: 013404.
18 Plaja, L. and Roso, L. (1993). *J. Mod. Opt.* 40: 793.
19 Plummer, M. and Noble, C.J. (2000). *J. Phys. B* 33: L807.
20 Plummer, M. and Noble, C.J. (2002). *J. Phys. B* 35: L51.
21 Fomichev, S.V., Zaretsky, D.F., Bauer, D., and Becker, W. (2005). *Phys. Rev. A* 71: 013201.
22 Fomichev, S.V., Popruzhenko, S.V., Zaretsky, D.F., and Becker, W. (2003). *J. Phys. B* 36: 3817.
23 Fomichev, S.V., Popruzhenko, S.V., Zaretsky, D.F., and Becker, W. (2003). *Opt. Express* 11: 2433.
24 Fomichev, S.V., Popruzhenko, S.V., and Zaretsky, D.F. (2003). *Laser Phys.* 13: 1188.
25 Oleinikov, P.A., Platonenko, V.T., and Ferrante, G. (1994). *J. Exp. Theor. Phys. Lett.* 60: 246.
26 Ganeev, R.A. (2012). *J. Mod. Opt.* 59: 409.
27 Gilbertson, S., Mashiko, H., Li, C. et al. (2008). *Appl. Phys. Lett.* 93: 111105.
28 Milošević, D. (2007). *J. Phys. B* 40: 3367.
29 Frolov, M.V., Manakov, N.L., Sarantseva, T.S. et al. (2009). *Phys. Rev. Lett.* 102: 243901.
30 Ivanov, A. and Kheifets, A.S. (2008). *Phys. Rev. A* 78: 053406.
31 Platonenko, V.T. (2001). *Quantum Electron.* 31: 55.
32 Frolov, M.V., Manakov, N.L., Sarantseva, T.S., and Starace, A.F. (2011). *Phys. Rev. A* 83: 043416.
33 Morishita, T., Le, A.-T., Chen, Z., and Lin, C.D. (2008). *Phys. Rev. Lett.* 100: 013903.
34 Strelkov, V.V., Khokhlova, M.A., and Shubin, N.Y. (2014). *Phys. Rev. A* 89: 053833.
35 Ganeev, R.A., Strelkov, V.V., Hutchison, C. et al. (2012). *Phys. Rev. A* 85: 023832.
36 Paul, P.M., Toma, E.S., Breger, P. et al. (2001). *Science* 292: 1689.
37 Tzallas, P., Charalambidis, D., Papadogiannis, N.A. et al. (2003). *Nature* 426: 267.
38 Antoine, P., L'Huillier, A., and Lewenstein, M. (1996). *Phys. Rev. Lett.* 77: 1234.
39 Facciala, D., Pabst, S., Bruner, B.D. et al. (2016). *Phys. Rev. Lett.* 117: 093902.
40 Strelkov, V.V. (2016). *Phys. Rev. A* 94: 063420.

41 Watson, J.B., Sanpera, A., Chen, X., and Burnett, K. (1996). *Phys. Rev. A* 53: R1962.
42 Zhai, Z., Zhu, Q., Chen, J. et al. (2011). *Phys. Rev. A* 83: 043409.
43 Chen, J., Wang, R., Zhai, Z. et al. (2012). *Phys. Rev. A* 86: 033417.
44 Zhao, D., Jiang, C., and Li, F. (2015). *Phys. Rev. A* 91: 033414.
45 Paul, P.M., Clatterbuck, T.O., Lynga, C. et al. (2005). *Phys. Rev. Lett.* 94: 113906.
46 Nubbemeyer, T., Gorling, K., Saenz, A. et al. (2008). *Phys. Rev. Lett.* 101: 233001.
47 Shvetsov-Shilovski, N.I., Goreslavski, S.P., Popruzhenko, S.V., and Becker, W. (2009). *Laser Phys.* 19: 1550.
48 Landsman, A.S., Pfeiffer, A.N., Hofmann, C. et al. (2013). *New J. Phys.* 15: 013001.
49 Yuan, X., Wei, P., Liu, C. et al. (2015). *Appl. Phys. Lett.* 107: 041110.
50 Ganeev, R.A., Suzuki, M., Baba, M. et al. (2006). *Opt. Lett.* 31: 1699.
51 Milošević, D.B. (2006). *J. Opt. Soc. Am. B* 23: 308.
52 Redkin, P.V., Kodirov, M.K., and Ganeev, R.A. (2011). *J. Opt. Soc. Am. B* 28: 165.
53 Haessler, S., Elouga Bom, L.B., Gobert, O. et al. (2012). *J. Phys. B* 45: 074012.
54 Mauritsson, J., Johnsson, P., Martens, R.L. et al. (2004). *Phys. Rev. A* 70: 021801.
55 Mairesse, Y. and Quéré, F. (2005). *Phys. Rev. A* 71: 011401.
56 Suzuki, M., Baba, M., Ganeev, R.A. et al. (2006). *Opt. Lett.* 31: 3306.
57 Rosenthal, N. and Marcus, G. (2015). *Phys. Rev. Lett.* 115: 133901.
58 Fareed, M.A., Strelkov, V.V., Thiré, N. et al. (2017). *Nat. Commun.* 8: 16061.
59 Krausz, F. and Ivanov, M. (2009). *Rev. Mod. Phys.* 81: 163.
60 Corkum, P. and Krausz, F. (2007). *Nat. Phys.* 3: 381.
61 Haessler, S., Strelkov, V., Elouga Bom, L.B. et al. (2013). *New J. Phys.* 15: 013051.
62 Wu, M., Chen, S., Camp, S. et al. (2016). *J. Phys. B* 49: 062003.
63 Haessler, S., Caillat, J., and Salières, P. (2011). *J. Phys. B* 44: 203001.
64 Salières, P., Maquet, A., Haessler, S. et al. (2012). *Rep. Prog. Phys.* 75: 062401.
65 Ferré, A., Boguslavskiy, A.E., Dagan, M. et al. (2015). *Nat. Commun.* 6: 5952.
66 Ganeev, R.A., Witting, T., Hutchison, C. et al. (2013). *Phys. Rev. A* 88: 033838.
67 Kulagin, A., Kim, V.V., and Usmanov, T. (2011). *Quantum Electron.* 41: 801.